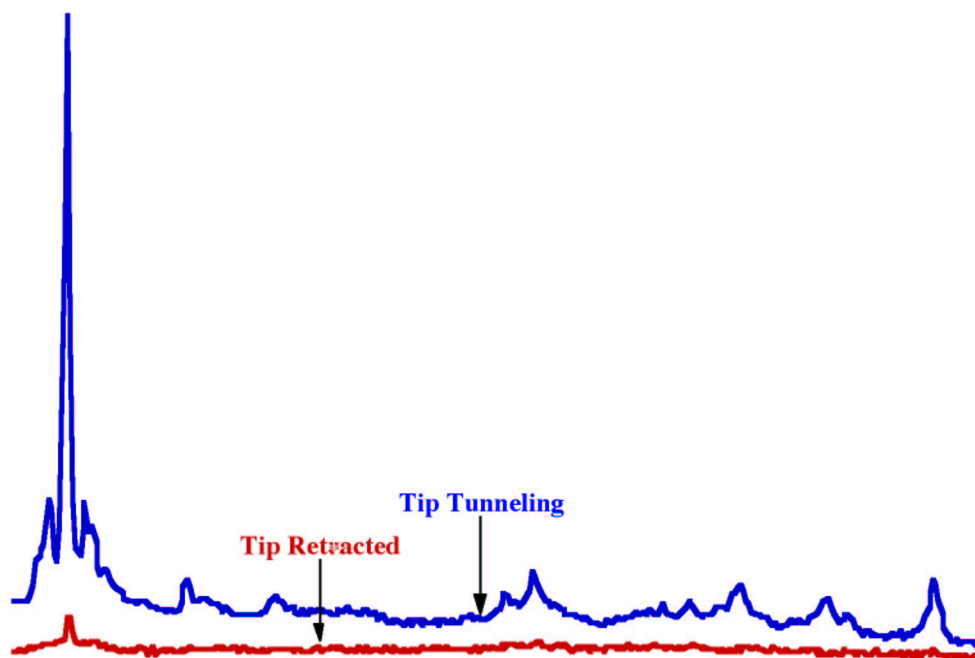# 4.   TIP ENHANCED RAMAN SPECTROSCOPY

4

4.1   Brilliant Cresyl Blue

The enhancement of the Raman signal due to the external contribution of an illuminated metal tip with sub-wavelength dimensions of the apex has been studied for different molecules adsorbed at both smooth and rough surfaces.

At smooth surfaces, molecules showing normal Raman scattering (NRS) will barely be seen. For convenience and for comparison of spectra and intensities, molecules with large Raman cross sections are the preferred light scatterers. A dye, brilliant cresyl blue (BCB), was chosen as the first test molecule. Organic dyes are rather large molecules with an extended frame of delocalized π-electrons. Due to the richness of energy levels present, often, electronic transitions are accessible, which cover a broad region in the visible frequency range. In the Raman process, the more resonant is the electronic excitation, resulting in an increasing lifetime of the excited state, the larger is the transition probability (see also Fig. 2.1 and corresponding discussion). The overall cross section for a resonant Raman scattering (RRS) may be many orders of magnitude higher than for the normal Raman process [101–108].

BCB shows the ideal absorption pattern for our purpose: as Fig. 4.1 illustrates, its fluorescence is effectively excited by the red laser light ($\lambda = 632.8$ nm). The fluorescence spectrum was obtained by passing the laser light through a cuvette filled with a (deeply blue coloured) 10^{-4} M BCB solution and recording in the back scattering mode. The dashed portion of the curve is the region cut off by the holographic notch filter; a three component (644 nm, 667 nm and 707 nm) gaussian fit in the energy scale reproduces the spectral feature and was used to extrapolate
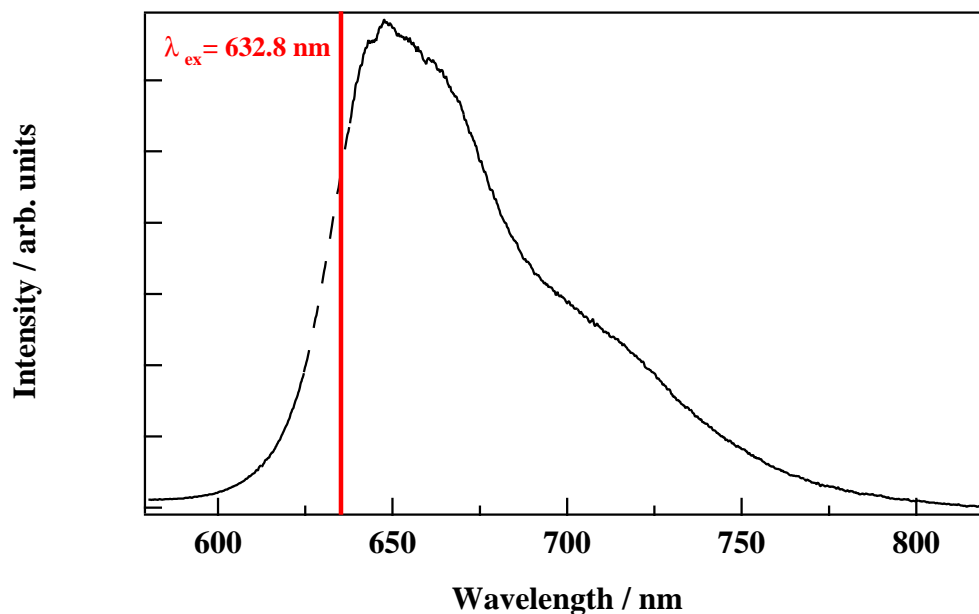
Figure 4.1: Fluorescence spectrum of Brilliant Cresyl Blue (BCB) recorded in the back scattering mode. Integration time: 1 s, laser power: 0.01 mW, $\lambda = 632.8$ nm, concentration of the dye in the water solution: 10^{-4} M.

the missing part. From the main fluorescence peak located at around 650 nm it can be estimated that the maximum absorption for the dye is roughly at 610 nm. A large resonance contribution for the Raman process will be present using a red laser for excitation. Still, in Fig. 4.1 no Raman bands are discernable. The reason is that fluorescence and Raman scattering are actually two competitive electronic processes, where fluorescence is superior because of its much larger cross section. Raman scattering is the faster process, excitation and de-excitation occur nearly simultaneously, but there is no real occupation of an excited state. Therefore, the relative cross sections are low ($\sim 10^{-30}$ cm^2 sr^{-1}). Excitation of the fluorescence occurs initially *via* the same excited state(s), but then the excited electron relaxes into a state with a longer lifetime, which is radiative. This can lead to higher cross sections for the fluorescence (up to 10^{-16} cm^2 sr^{-1}). Suppression of the fluorescence takes place if the dye is adsorbed on metal substrates: the energy transfer from the excited molecule to the metal (see Fig. 2.2 and related discussion in the text)

is much faster than the fluorescent decay. Thus, in the TERS experiments, the presence of a metal film onto which the molecules are deposited offers the additional and very valuable advantage of (selective) fluorescence quenching.
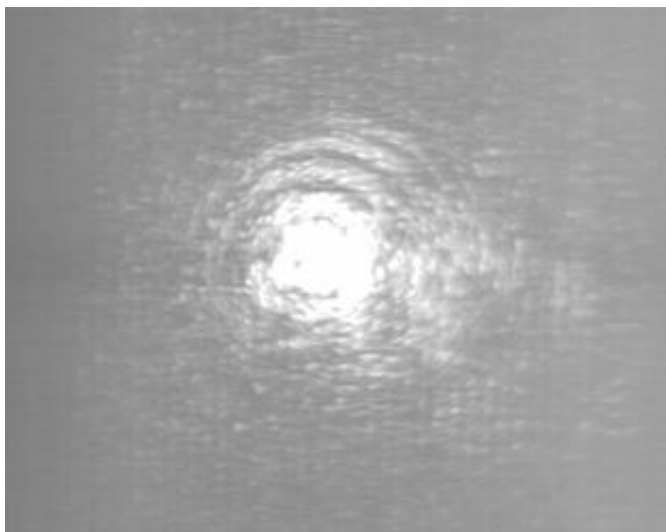

Figure 4.2: Even if the real position of the tip apex is hardly seen in the white light, the interference fringes formed by the laser light impinging on the tip may be used as an indication for a good alignment.

As can be easily understood, the adjusting of the laser spot with respect to the tip is of paramount importance. With the sample and tip illuminated from below (through the glass slide and through the thin metal film), an helpful feature may be seen on the auxiliary camera used for the sample surface monitoring. The monochromatic light scattered by the tip forms circular interference patterns (Fig. 4.2) when the apex is exactly found in the center of the laser spot. The brighter and darker rings stretch in or out when the height of the tip is changed from the tunneling distance to the at-rest position or *vice versa*. Considering the light wavelength and the distance by which each ring is moved, it is possible to estimate the vertical excursion of the tip (roughly 1000 nm) when switching between the two positions.
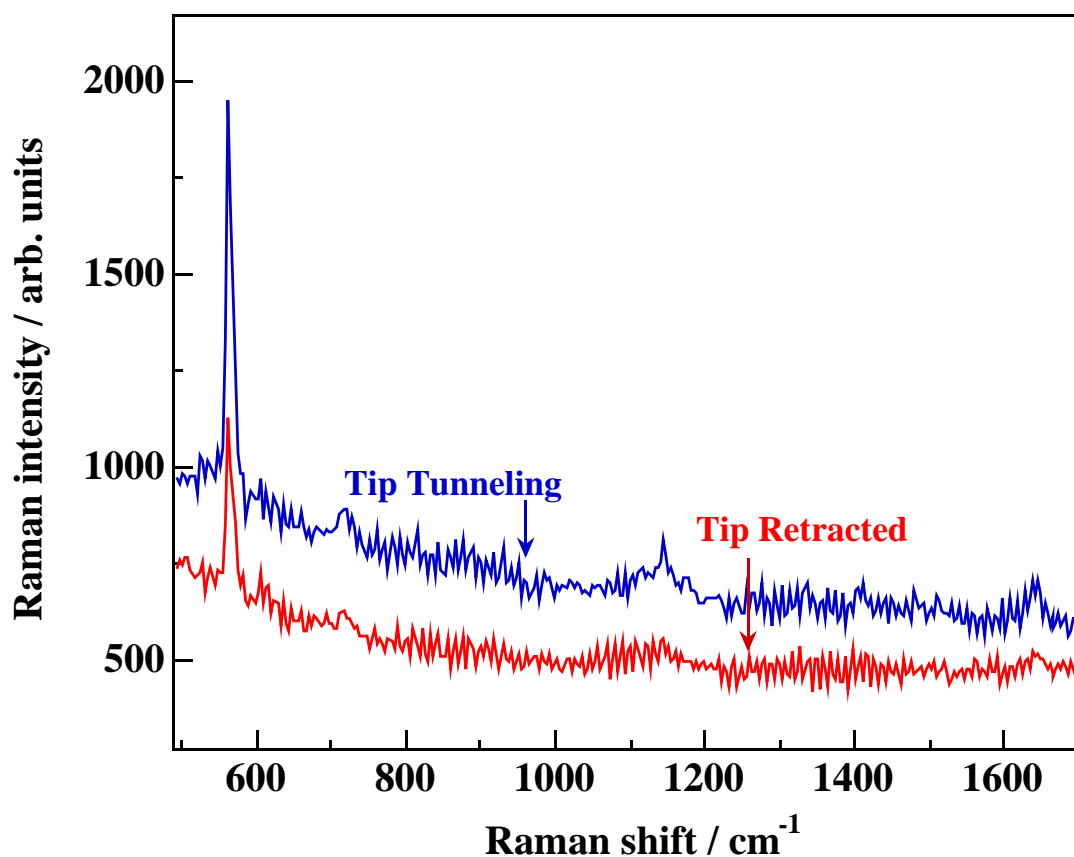
Figure 4.3: Comparison of the (resonance) Raman spectra for Brilliant Cre-syl Blue adsorbed at a smooth gold surface with the illuminated silver tip at tunneling distance and retracted above the metal surface. Integration time for each spectrum was 100 s, the laser power at the sample 1 mW. The spectra, taken with a 50x magnification objective, refer to the same focal area and were sequentially taken.

Our first experiments on the tip enhancement of the Raman signal were per-formed on smooth, 12 nm thick gold films covered with a few layers of BCB, using a silver tip and an inverted 50x objective. Two spectra are shown in Fig. 4.3, labelled as tip retracted and tip tunneling. These labels should be, in a way, un-derstood as the near field associated with the metal tip acting on the substrate or not. During the experiment the laser spot is carefully focused below the tip and Raman spectra are alternatively recorded with the tip in the tunneling posi-tion (the feedback for the current adjustment is on, set value: 1 nA with a bias

of 50 mV positive with respect to the tip) and with the tip far away from the surface (feedback off, corresponding to the maximum compression of all the piezo elements). The observed enhancement has to be ascribed solely to the near field of the tip since a higher Raman intensity is always seen when the tip is found at the tunneling distance, while the lower signal is promptly re-established should the tip be moved away. An estimation of the signal increase may be carried out considering the integral intensity of the predominant band found at 570 cm^{-1}, most likely assignable to some skeletal stretching mode of the carbon molecular frame. This value is plotted against the number of continuous spectral acquisition in Fig. 4.4. Each single acquisition took 100 s, so that the the same area was illuminated for almost 20 minutes. Such a long continuous exposure to the focussed light has as a consequence the bleaching of the dye. This term is used to describe the photo-activated process causing a molecule to lose part of its optical properties (in our case the optical resonance at $\lambda = 632.8$ nm) due to the breaking and rearrangement of some bonds into a new, non resonant, fragment. Indeed, it is seen that both curves in Fig. 4.4 have negative slopes, since the intensity of the Raman signal is directly affected by the decrease of the resonant contribution. The obvious reason for the steeper slope of the red curve is the higher field localized below the tip that accelerates the degradation of the dye. TERS, due to its nature, acts only on the molecules underneath the tip. Therefore, a small decrease in the total number of scattering molecules barely affects the SERS signal, while most of the TERS is lost with time. The two curves merge together when none of the molecules is affected by the tip field.

In all the TERS measurements carried out with the BCB dye, special care was taken to avoid tip contamination. It was noted in the early measurements, when either a thick layer of the dye was deposited on the film or after an unintentional contact of the tip with the metal surface during the approach, that huge Raman spectra could be obtained in the tip tunneling position, which were by far much more intense than those shown in Fig. 4.3. The silver tip represents, in a way,
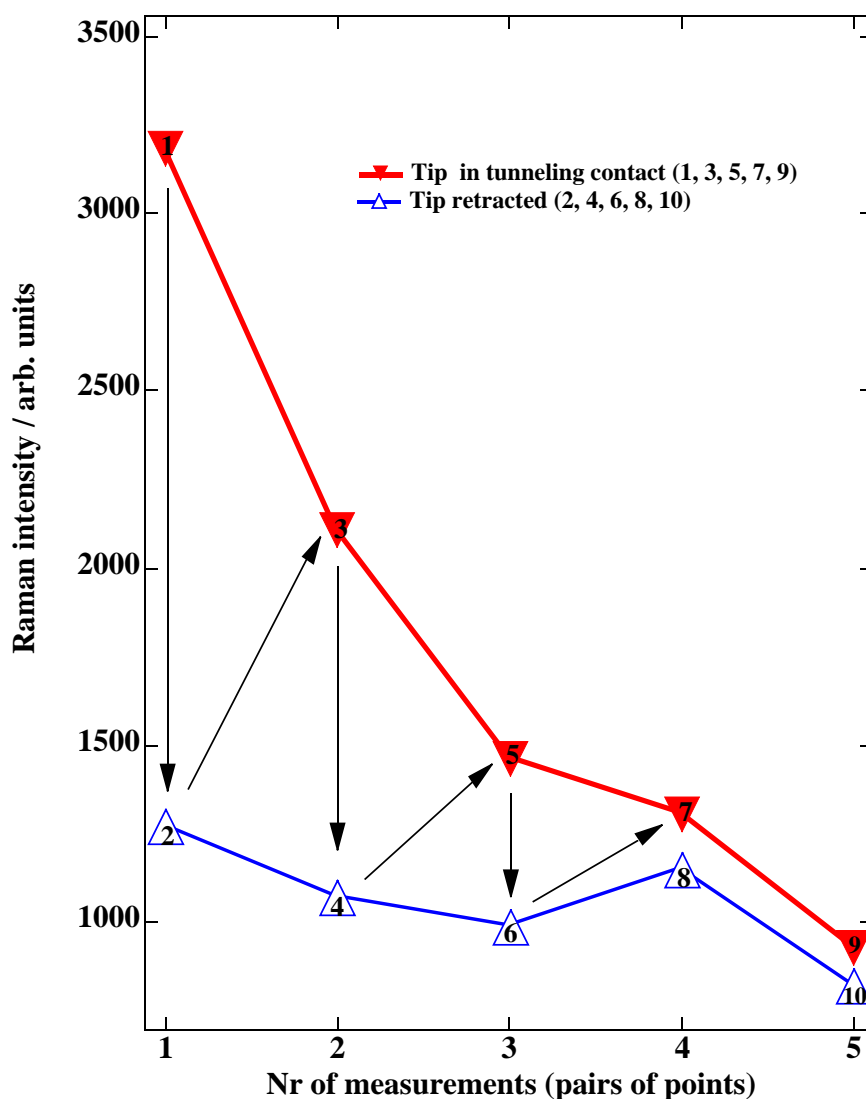
Figure 4.4: The Raman intensity for the BCB main band at 570 cm^{-1} is plotted against the number of the spectral acquisition (100 s for each acquisition) during a single experiment for the two configurations: tip tunneling and tip retracted. The laser power at the smooth gold sample was 1 mW.

the perfect SERS substrate,[6] having not only a very sharp apex generating the tip enhancement, but being formed along the etched walls of many granular stuctures, structures that do not contribute significantly to the tip enhanced signal (and

---

[6]SERS studies where a tip is used as substrate for single molecule detection (SMD) are already carried out in the group of Prof. X.F. Liu at the university of Beijing (private communication).

neither to the tunneling current). Since the electromagnetic enhancement scales quickly with the distance from the LSP mode supporting metal, an adsorbate at the tip receives an higher enhancement than a molecule located only a few $\mathring{A}$ away. The former signal, if present, will overwhelm any information from the surface.

Clearly, our attempts are devoted to developing a new technique where the field enhancement is given for species not directly adsorbed at the enhancing unit. In order to have only TERS for the adsorbate at the metal film and *not* SERS for species contaminating the tip, any contact of the tip with the surface must be carefully avoided; should this happen, the tip is discarded. Also, to prevent the tip diving into a thicker dye layer while approaching, monolayer quantities of the dye are dispersed onto the film. These precautions may be still not enough: it was found more convincing, after any successful tip enhancement measurement, to take Raman spectra directly from the tip after removing the film and check for any contamination of the dye. As mentioned before, also very small traces of the dye on the silver tip may yield very intense Raman spectra. Should the recorded spectra from the tip bear no resemblance to the dye reference spectrum, a contamination may be ruled out. The vibrational spectra of BCB adsorbed at either gold or silver show no discernable difference (apart from the higher intensity observed for silver) which makes it rather difficult to rule out an eventual tip contamination *in situ*. This will not be the case for cyanide ions. It is also noteworthy that we observed several times spectra from the tips which are astonishingly rich with intense and fluctating carbon bands, thereby also illustrating the extremely high SERS activity of etched tips. In a separate paragraph, the somewhat tedious and almost unavoidable problem of carbon contamination is addressed.

Regarding the bleaching of the dye in the focal spot, an easy way to limit this drawback is to lower the laser power with filters. By doing so, also the intensity of the, already weak, Raman signal may decrease below the detection limit. A stronger signal is then needed and a mild activation of the gold surface may provide it. Such mildly roughened films were prepared by depositing a few layers of gold onto the evaporated metal. They yield spectra of high quality (see bottom curve of Fig. 4.6) even in a shorter integration time and using a lower laser power, because
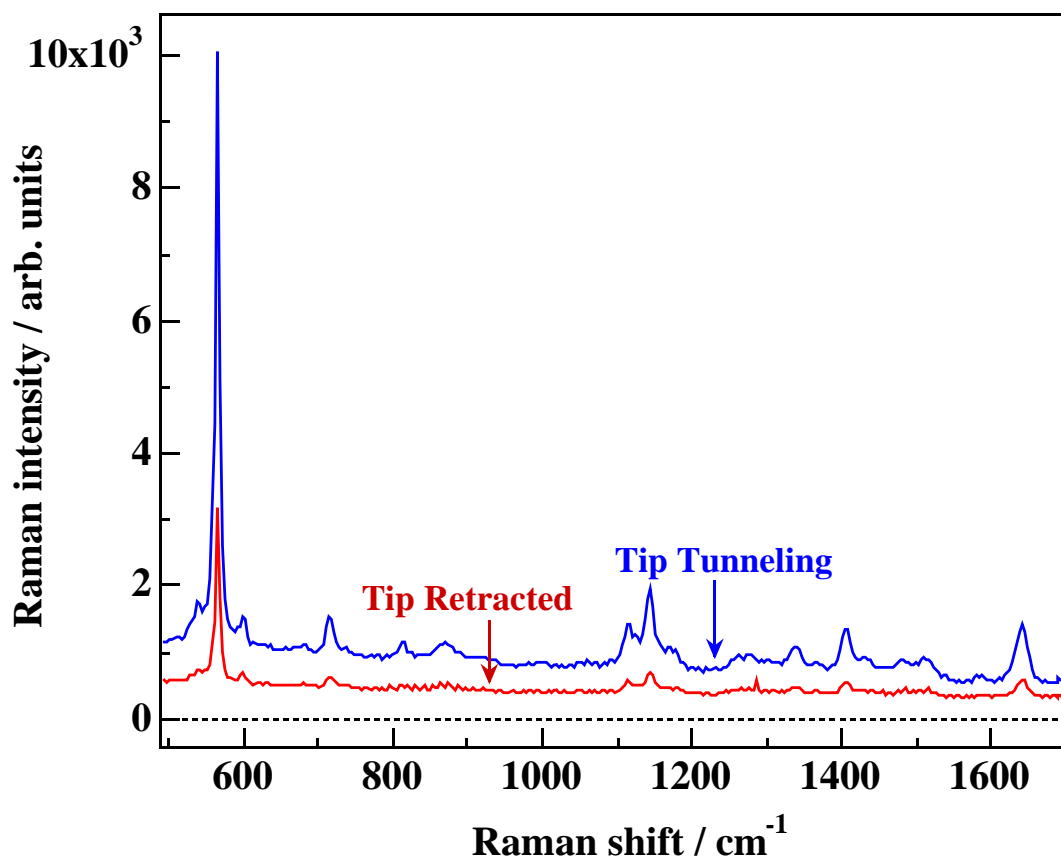
Figure 4.5: SERS and TERS spectra for the BCB dye molecule adsorbed on a mildly activated, *i.e.*, roughened gold film. Integration time: 50 s, laser power: 0.1 mW, 50x magnification.

of the presence of some surface enhancement (SERS). Yet, there is in addition a tip enhancement, observable now for all the Raman bands. Moreover, longer lasting measurements can be performed. As seen in Fig. 4.6, the bleaching, while still present, is not as dramatic as shown in the experiment before, (the red curve in Fig. 4.4).

It may be found somewhat puzzling to have TERS and SERS at the same time or, in other words, for twice the electromagnetic enhancement: from the gold surface and, additionally, from the silver tip. In both cases the enhancement is given by subwavelength structures for molecules located close enough to them. These active *hot spots* represent only a minor proportion of the surface and it is likely
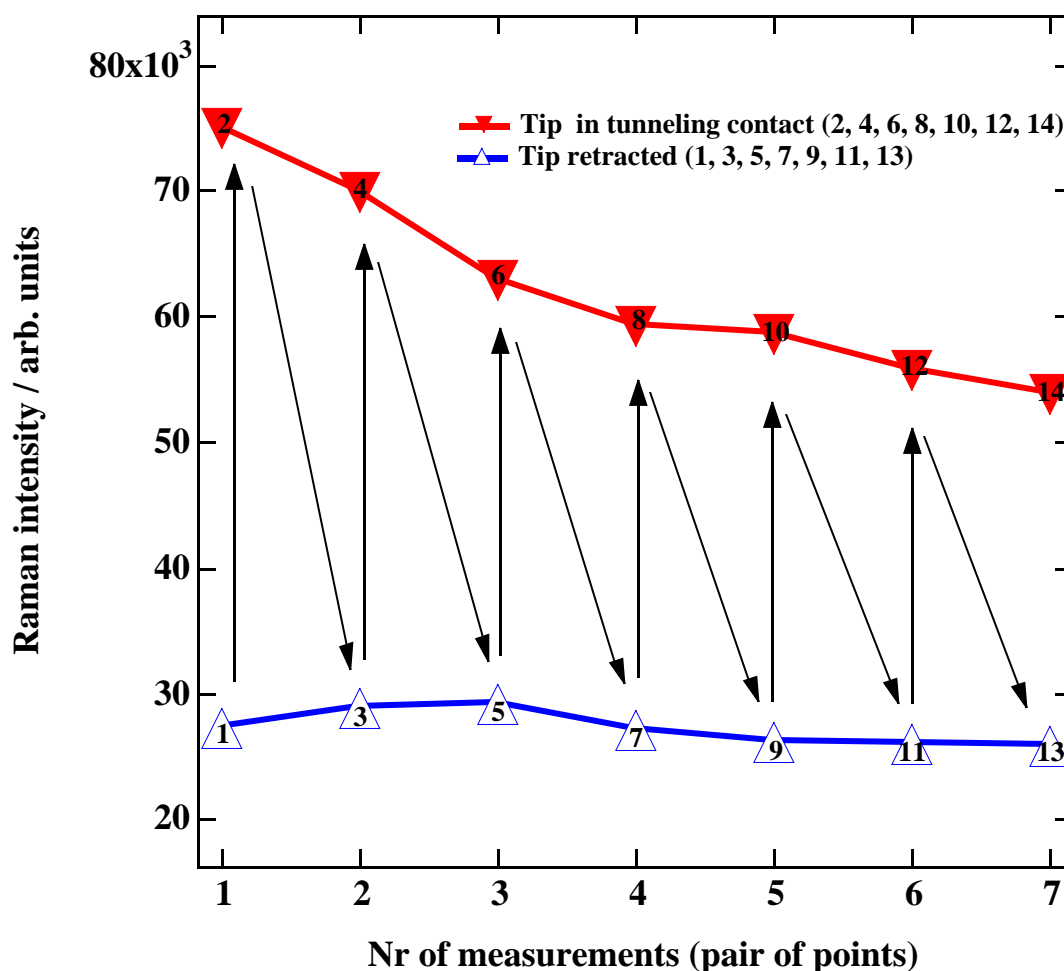
Figure 4.6: The Raman intensity for the BCB main band at 570 cm^{-1} plotted against the number of spectral acquisitions (50 s for each acquisition) during a single experiment for the two configurations: tip tunneling and tip retracted. The laser power at the roughened gold sample was 0.1 mW.

that the tip picks up a less active environment (in terms of SERS) still providing a superior enhancement; thus, the total signal increases. A granular substrate for TERS experiments has also been used by other authors [68, 109–111] for the same need to have a faint starting signal and with similar results. Comparing all the enhancements obtained with different silver tips[7] on gold surfaces (either smooth

---

[7]Not all the tips provide the same enhancement. The plasmon modes localized below the tip must be excited by the laser light in order to produce the enhanced field. The LSP resonances

or roughened), the highest signal increase (always considering the band at 570 cm^{-1}) ranges between a factor of 3 and 4. The net ratio between the intensities of the two signals may be defined as an apparent enhancement. Since the size of the tip, *i.e.*, the near-field area generated by the tip, is much smaller than the laser spot, taking in account the ratio between them, the actual tip enhancement may be estimated[8] to be at least three orders of magnitude and up to 10^4, considering a tip size of 40 nm and a spot size of 2000 nm for the 50x magnification or 1000 nm for the 100x magnification. Indeed TERS experiments with the dye have been carried out also using an objective with higher magnification, 100x. While with the 50x magnification objective a roughly four fold higher signal was observed, the tip enhanced signal in Fig. 4.7 is almost 16 times more intense. The observed intensity rise should scale reciprocally with the area of the laser focus, while the actual tip enhancement and SERS remain more or less the same, being unaffected by the magnification optics used, not considering (slightly) different numerical aperture effects.

Before presenting TERS for cyanide ions we point out a further experimental observation made from the tip enhanced spectra of the BCB molecule. In order to appreciate more clearly this feature, detected also by Kawata *et al.* [68, 109–111], more spectra are reported in the full range. Not only the Raman bands have increased intensities but also the baseline is shifted upwards upon approaching of the tip. The broad feature centered at around 2800 cm^{-1} should not be considered since it is due to the fluorescence of one of the elements in the optical path (most likely the notch filter). A first tentative explanation for this result could be an enhancement of the fluorescence from the dye always provided by the near field of the tip.

---

are defined by the size, shape and orientation of the tip apex (or, more properly, of the grain found at the apex). Not surprisingly in many experiments no enhancement at all was observed: the tip grain size was not suitable to the used wavelength or, *vice versa*, the incident light did not match the resonances supported by the tip.

[8]Using the tip size as an indication of the tip field is only a simple approximation; much smaller localization length and consequently larger enhancement factors are obtained if making use of the formula $L = \sqrt{2rd}$.
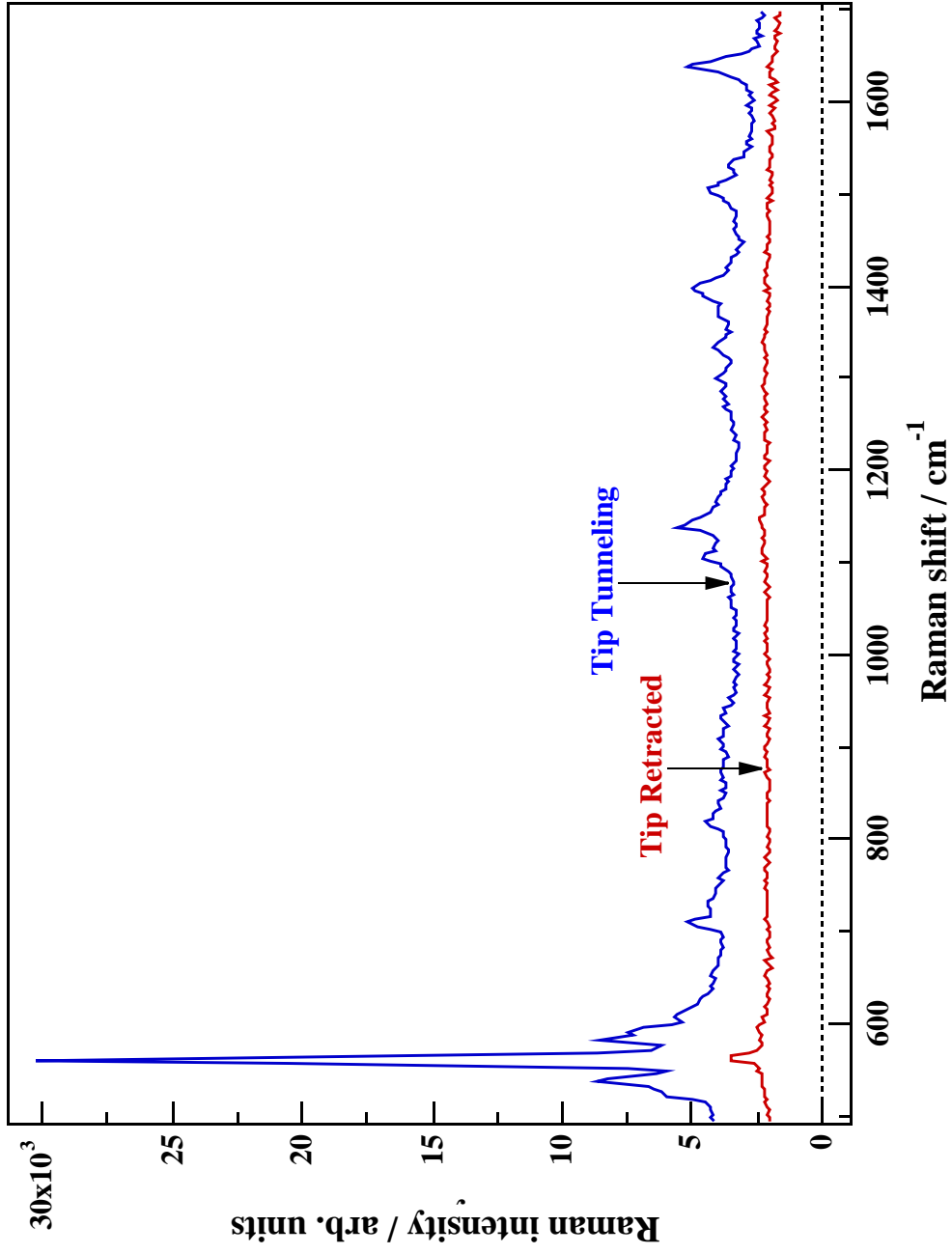
Figure 4.7: Resonance Raman spectra for Brilliant Cresyl Blue adsorbed at a smooth gold surface. All parameters similar to those reported for Fig. 4.3, apart from the objective: 100x magnification.
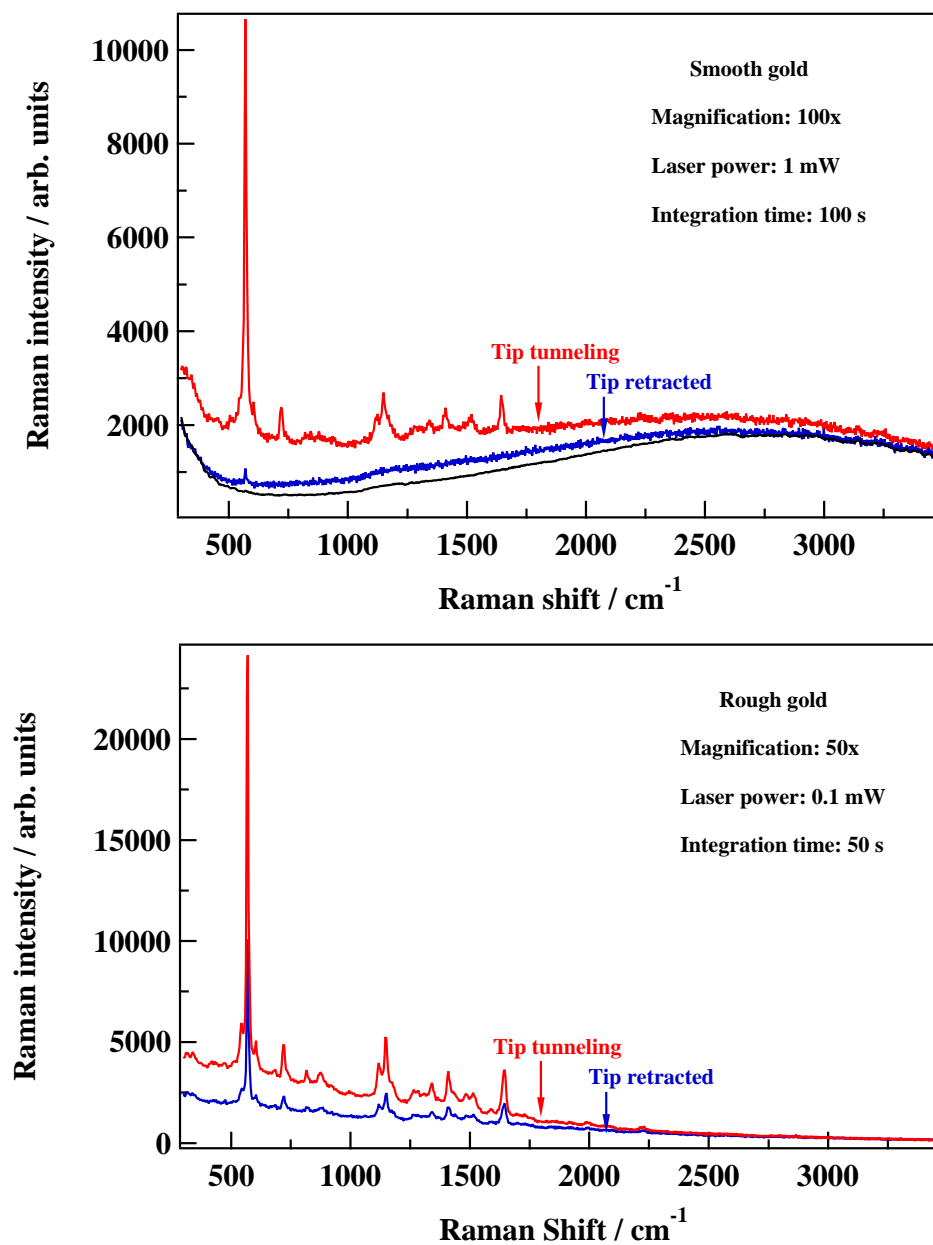
Figure 4.8: The enhancement of the Raman signal by the silver unit is always accompanied by a remarkable increase of the background. In the upper plot the instrument background signal, obtained by focusing the laser spot on a portion of the gold film where the dye was not deposited, is also reported.

Indeed, the wavenumber region in which the continuous rise of the background is observed corresponds well, in the wavelength scale, to the right wing of the BCB fluorescent emission seen in Fig. 4.2. By subtracting from both spectra the signal obtained from the clean gold film, it is possible to evaluate the net enhancement for the fluorescence, which is roughly four times (100x magnification) or two times (50x magnification) weaker than the reported value for the Raman bands. The fluorescence and Raman scattering may be differently enhanced by the silver unit since molecules in different chemical enviroments[9] are involved in the two processes and the enhanced field generated by the tip is spatially inhomogeneus. Fluorescence may be not the only source of the continuous signal enhanced by the tip. The metal unit acts as an additional light scattering element present in our system when the feedback loop is closed and the resonant excitation of localized plasmons may have different outcomes. Coupling of these modes, *e.g.,* with phonons in the metal may lead to a continuous radiative emission centered around the laser light.[10]

---

[9]For the few molecules in a partly filled second adsorbate layer the energy transfer taking place with the metal is already less favorable and they will contribute less to the Raman scattering, but more to the fluorescence.

[10]Experiments in the Anti-Stokes region are needed to test this hypothesis or the fluorescence enhancement.

4.2   Cyanide

The applicability of TERS was also explored with a much more familiar adsorbate. There were a few challenging reasons for choosing cyanide ions at gold as another test system for the tip enhancement: no resonant effects are present at $\lambda_{ex} = $ 632.8 nm, the unenhanced Raman cross section of the unbound CN^- molecule is extremely low; CN^- is rather similar to the isoelectronic CO molecule, the other small molecule with which surface science deals so often. No bleaching effects are expected. The CN^- stretching mode frequencies for the molecule bound either at silver or gold surfaces are well separated [112–117]. Therefore, using a silver tip and a gold film, the assignment of the source of the signal is straightforward. Moreover, this diagnostic band falls in an energy region that is not obscured by the intense and randomly fluctating bands found when carbon contamination is present.

Substrate	δ (M-C-N)	ν_1 (M-CN)	ν_2 (C-N)
Ag	256	411	2168
Au	288	383	2131

Table 1: Mode assignments in wavenumbers (cm^{-1}) for cyanide ions adsorbed at gold and silver SERS active substrates [112].

Reference spectra for CN^- ions adsorbed at massively roughened gold and silver electrodes are reproduced in Fig. 4.9. They were recorded in air after emersion of the electrode from the cyanide solution where they were kept polarized at -750 mV *vs.* SCE. All the characteristic frequencies are listed in Tab.1. The strongest peak is the C-N stretching vibration. At lower wavenumbers, the much weaker bands assigned to the bending vibration and the second stretching mode (Me-CN) are found. To appreciate more clearly the low frequency region, the Stokes and anti-Stokes branches, symmetric with respect to the laser line at zero wavenumber, are shown in the inset.
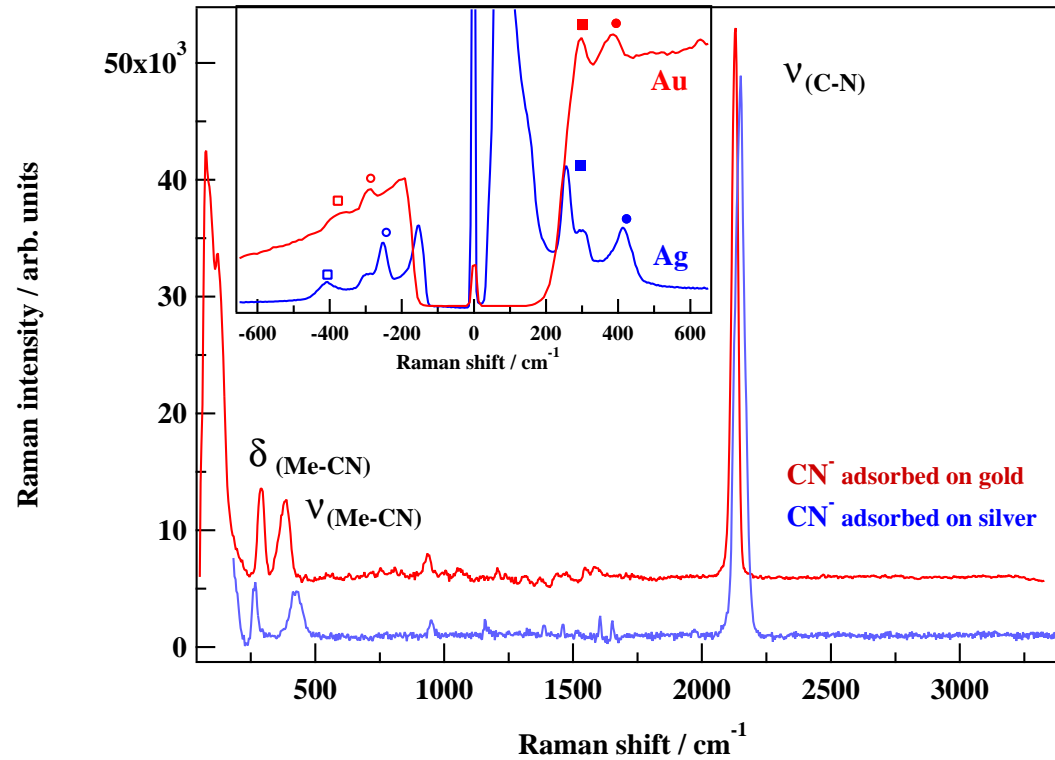
Figure 4.9: SER spectra of cyanide ions adsorbed at massively roughened gold and silver substrates. The electrodes were polarized at -750 mV *vs.* SCE in a 10^{-3} M NaCN solution also containing 10^{-1} M KClO$_4$ as supporting electrolyte and then emersed for recording in air. Integration time was 5 s with 1 mW laser power available at the sample. In the inset: the same samples and recording conditions hold, apart from the grating position. The Stokes and anti-Stokes region are both reported: the bending modes are indicated by squares and the first stretching mode by circles.

Other features discernible in the spectra may be assigned to a small amount of carbon contaminating the electrode (between 1200 cm^{-1} and 1600 cm^{-1}), to coadsorbed ClO$_4^-$ ions from the cyanide solution (900 cm^{-1}) and finally to metal-metal vibrations (below 100 cm^{-1}). Spectra were also taken *in situ* during the polarization of the electrode, see Fig. 4.10. CN$^-$ adsorption already starts at -300 mV for gold and at a slightly more negative potential for silver. The downward shift in the frequency of the main stretching vibration upon changing the electrode potential to more negative values is ascribed to the different electric field present at the liquid electrolyte/metal electrode interface that influences the stiffness of the bond.[11] In air, the frequencies are considerably shifted to higher wavenumbers, also due to the oxidation of the metals. CN$^-$ ions would make a perfect candidate should the TERS investigations also be carried out in an electrolyte solution where adsorption will take place both at the gold substrate and at the silver tip; by keeping the two metals at different polarization, the respective frequencies would be still separable.

The mild activation procedure of the gold substrate was definitely also needed for the CN$^-$ investigation in the inverted microscope configuration. The experiments were carried out in a similar way as described in the previous chapter: spectra from the same spot were taken alternatively with the tip in and out of the focus. Also for the cyanide ions the illuminated silver unit located at tunneling distance from the adsorbate covered gold film gave a strong contribution to the intensity of the Raman signal. The two spectra shown in Fig. 4.11 were taken under the same experimental condition as for Fig. 4.7: the integration time for each spectrum was 50 s and the 50x magnification objective was employed. There was no need to decrease the laser power since the CN$^-$ ions proved to be quite strongly bound at the surface; *i.e.,* there were no photon-induced bleaching effects, contrary to the case of the BCB dye.

---

[11]The metal ion complex formed at the surface is believed to be Me(CN)$_2^{(2-\lambda)-}$, with a partial positive charge on Me $\lambda = 0.8$. The CN group binds to the metal by donation from the antibonding $5\sigma^*$ orbital. By lowering the voltage also the partial charge is lowered and the σ^* donation decreases with the net effect of weakeaning the CN bond whose frequency moves to lower wavenumbers [114].
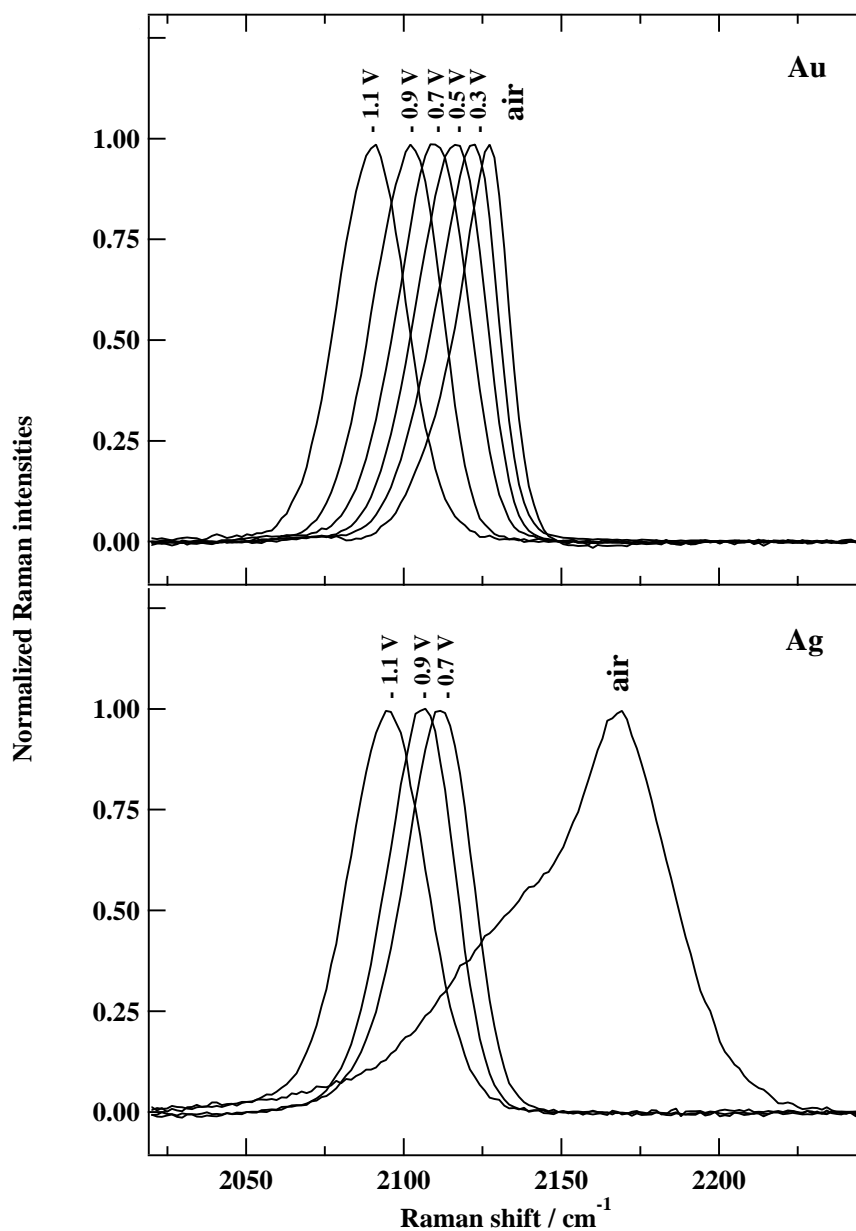
Figure 4.10: The shift in the position of the C-N stretching vibration for gold and silver electrodes upon changing the applied voltage *vs.* SCE. The aqueous solution contained 10^{-3} M NaCN and 10^{-1} M NaClO$_4$; a platinum wire was used as counter electrode.
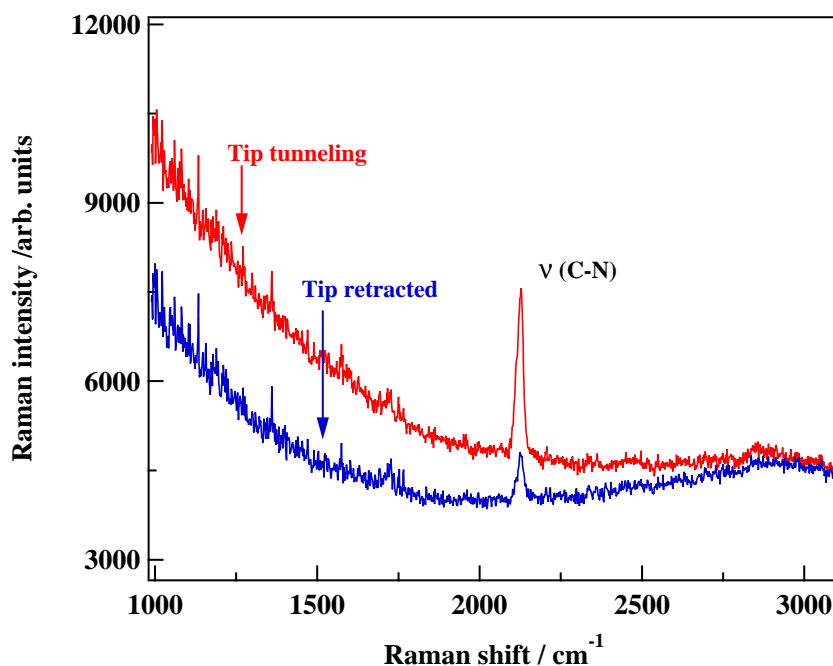
Figure 4.11: The increase in the intensity of the Raman band assigned to the stretching vibration of CN^- ions adsorbed on a mildly activated gold substrate upon approaching of the silver tip to the tunneling distance. Integration time: 50 s, laser power: 1 mW, 50x magnification.

Nevertheless, as depicted in Fig. 4.12, recording the peak intensities of the two signals over time, one with the tip retracted and the other with the tip tunneling, it becomes obvious that the enhancement is not constant. The thermal drift of the scanning tip has to be taken into account when tunneling for a long time, especially when the substrate is not atomically smooth, as was the case for our roughened gold film. The elapsed time to which Fig. 4.12 refers was almost 35 minutes and the lateral drift of our STM unit is in the range of 0.3 nm per minute. Thus, the observed variation in the tip enhancement is related to the movement of the the tip along a granular structure. Creeping above a small bump on the surface, the tip may move into an optimum (or just better) geometrical condition for the plasmons localization and thus, a stronger electromagnetic field is generated between the two protrusions for a limited time.
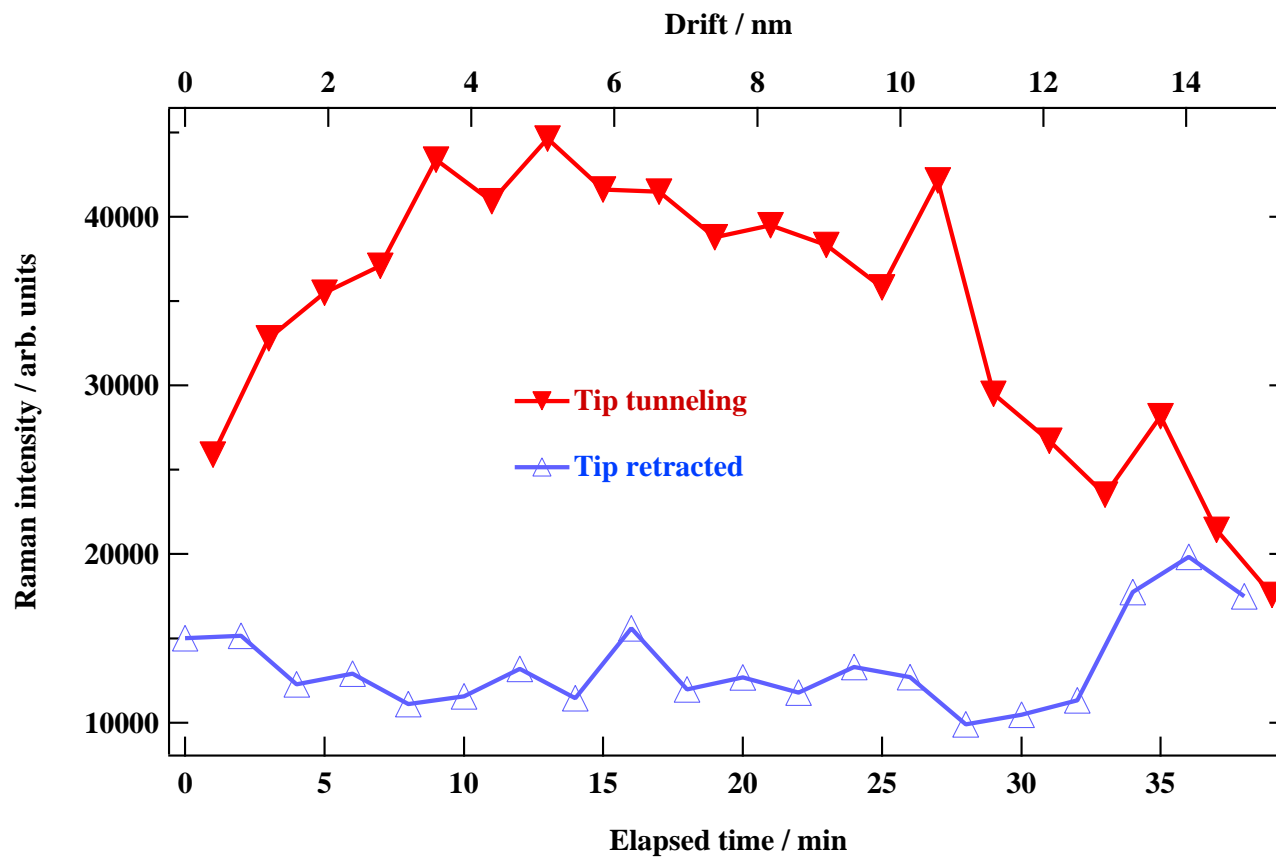
Figure 4.12: The Raman intensity for the CN stretch band is plotted against the elapsed time (50 s for each spectral acquisition/point) during a single experiment for the two configurations: tip tunneling and tip retracted. The laser power at the roughened gold sample was 0.1 mW.

In this sense, the upper curve of the figure may be considered as a trace of the surface topography taken in the Raman light.

In other experiments, an additional Raman band in the CN^- stretch region was observed for the silver tip in tunneling contact with the gold surface. For a convenient comparison, the normal SERS spectra for CN^- obtained (in air) from gold and silver electrodes after strong activation are shown in addition to the TERS results (Fig. 4.13). The frequency of the side band at 2168 cm^{-1} coincides well with the stretching frequency of CN^- adsorbed on silver. The appearance of a second peak when the silver tip "enters" into the focus indicates that we observed in this experiment (the rare case of) CN^- molecules adsorbed at the gold film and at the silver tip, at the same time. The first signal is externally enhanced by the tip, the second one, due to molecules directly adsorbed at the silver unit, is surface enhanced. Since no direct contact between tip and sample took place, the contamination of the silver tip by CN^- has to be ascribed to a single very close approach during the tunneling, in which a small fraction of CN^- ions was collected by the silver tip, located a few $\mathring{A}$ above the surface. The small inhomogenous broadening of the Raman band assigned to CN^-/silver is a further hint that this signal originates from only a very small number of molecules (compare this with the broad feature obtained from the massively roughened electrode where a large number of molecules distributed over a variety of different adsorption sites contributes to the broad band). More relevant is that the signal of the adsorbate at the surface still received the expected external enhancement. The low frequency modes, especially the metal-ion stretching vibration, are even more diagnostic of the metal surface, but these are much weaker in intensity and are usually not detected when using the thin film configuration, not even with the tip enhancement.

A different approach was then employed where the tip is directly illuminated from the side at an angle of 60° relative to the surface normal (Fig. 2.8). In this configuration, gold films, 250 nm thick, massively roughened, provided a much higher signal to noise ratio for the CN^- Raman signal. Once the tunneling contact between tip and metal surface is established, the side of the tip (and its reflected
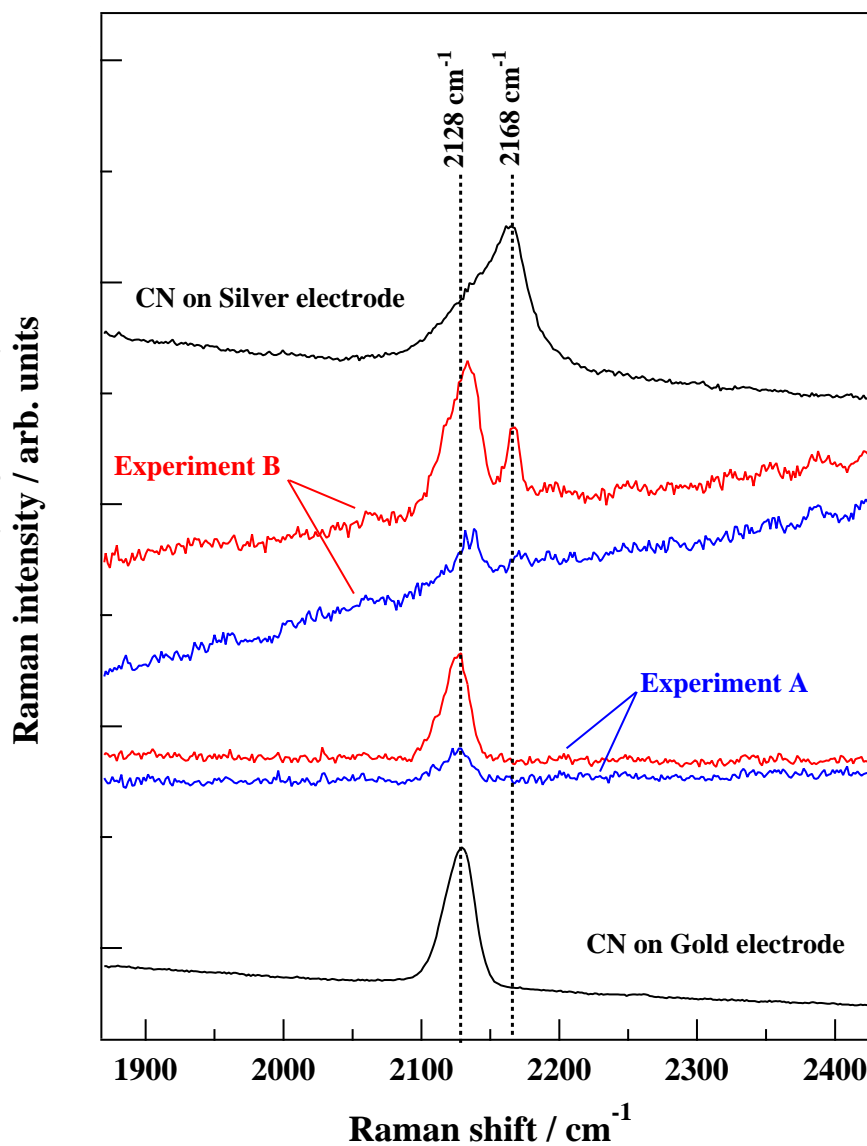
Figure 4.13: SERS and TERS for adsorbed CN^- ions. Top and bottom curves: SERS for silver and gold electrodes, respectively. Curves marked with "experiments A, B" (subsequent experiments at different locations of the film) are for CN^- ions adsorbed at a weakly activated 6 nm gold film, with the silver tip in the retracted or in the tunneling position. Laser power at the sample ca. 0.1 mW.

image on the metal film) is visualized in the white light on the secondary CCD camera. The STM platform is moved[12] until the junction is found in the laser spot (Fig. 4.14).
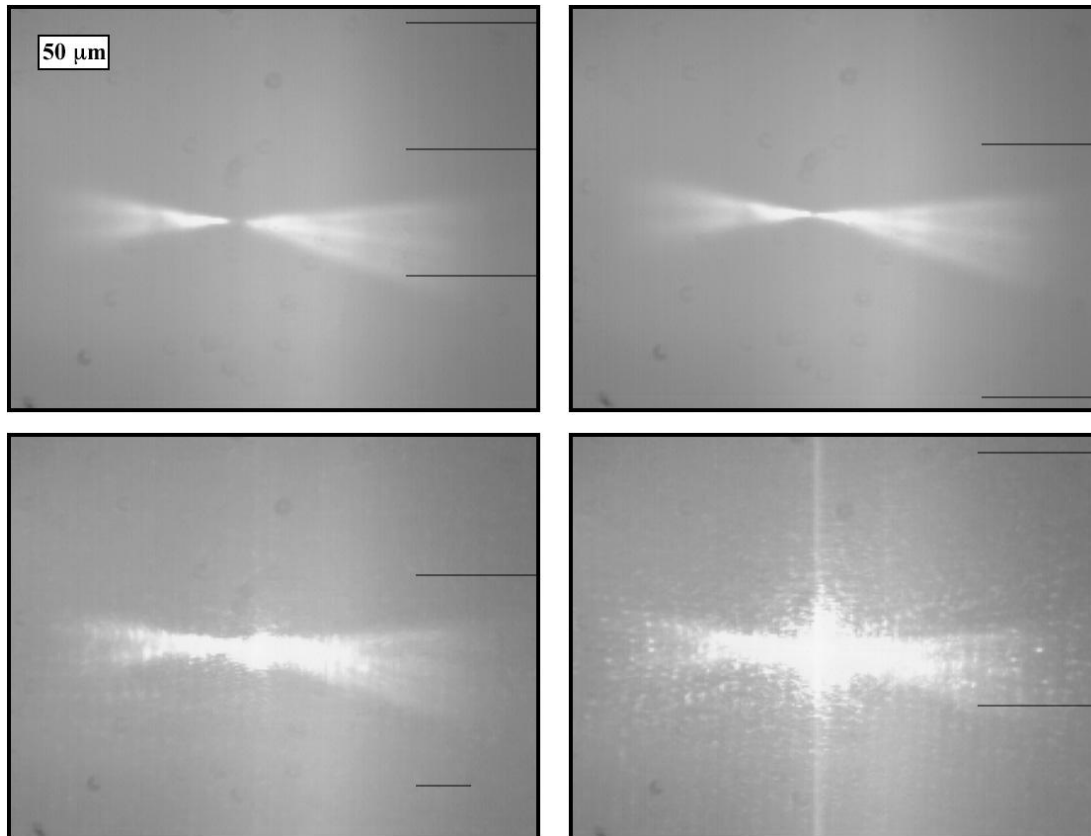

Figure 4.14: Image of a silver STM tip over a gold reflective surface taken with a 50x magnification objective forming an angle of 60° with the tip axis. On the right the tip is in tunneling contact with the surface; on the left in the retracted position. In the top row only the white light illumination is present; in the lower row the laser light is also passed trough the objective. With the tip in the tunneling position, the laser spot (due to the elastic light scattering) is much brighter.

---

[12]During the alignment the current feedback loop is not active and the tip is in the retracted position.

A tip enhancement of the Raman scattering was also observed with a side illumination of the metal unit. Fig. 4.15 shows a series of Raman spectra recorded using the 60° arrangement. The tip enhancement for the C-N stretching signal has on average a value of 7, higher than that observed with the former approach, where the tip was illuminated from below. In the second panel, carbon peaks in the range between 1400 cm^{-1} and 1700 cm^{-1} also appear in the tip tunneling curve. It is very difficult to assess whether these blinking features are due to carbonaceous fragments adsorbed on the illuminated tip or due to carbon adsorbed on the surface underneath, which also profits from the tip enhancement.

With a longer integration time (lower panel), the low frequency modes at 288 cm^{-1} (ν_{Au-CN}) and 383 cm^{-1} (δ_{Au-C-N}), characteristic of the metal surface/molecule bond, become clearly visible above the noise. Those frequencies also receive the expected external enhancement. No CN$^-$ ion contaminated the tip and, thus, no SERS contribution from the tip are to be suspected. An increase of the background is also observed in the case of TERS for the CN$^-$ system. Clearly, for the adsorbed ions no fluorescence is expected at the excitation wavelength. Therefore, the enhanced background may be ascribed to the already detected presence of carbonaceous species, including amorphous carbon. Even if the surface is mainly covered by the strongly bound CN$^-$ ions, the carbon spongy structures may bind to the metal at a few locations (pinholes) while the rest of it is not in direct contact with the metal and thus receive an higher fluorescence than Raman enhancement.

In the spectra it may also be noticed that the main peak position moved from 2133 cm^{-1} to 2131 cm^{-1}. These two different frequencies for SERS and TERS were reproducibly found in sequentially recorded spectra. Neither the static nor the dynamic electromagnetic fields are strong enough to cause Stark shifts. Cavity effects can be excluded due to the small number of molecules affected. The width and asymmetry of the SERS bands is due to the substantial inhomogeneous broadening upon averaging over contributions from different adsorption sites at the rough Au surface. Therefore, the peak shift is interpreted simply in terms of different weighting of the contributions of CN$^-$ adsorbates in different local environments to the overall Raman intensity, depending on the local magnitude of
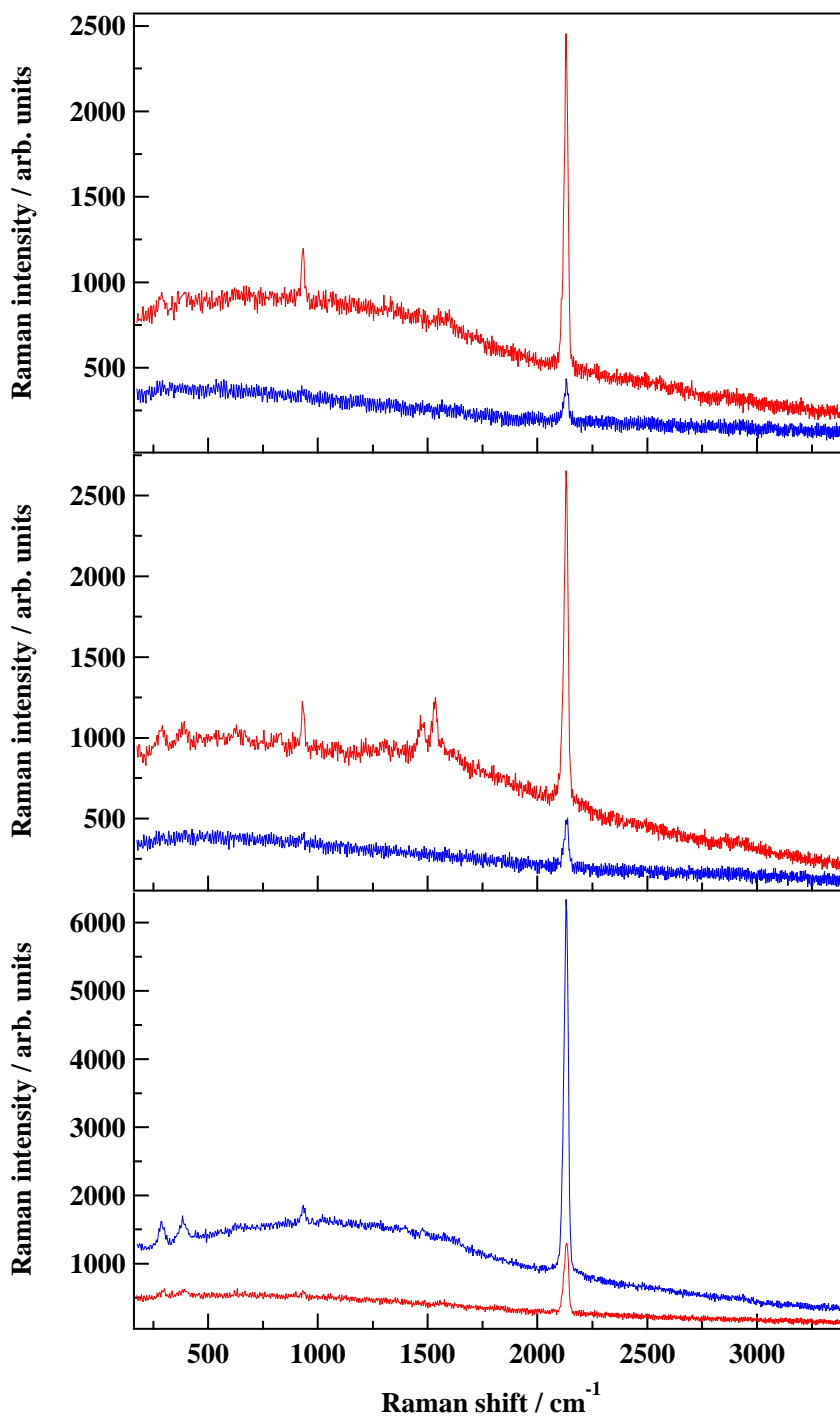
Figure 4.15: SERS and TERS spectra for CN^- ions adsorbed at a Au surface using the 60° approach and an electrochemically etched Ag tip. Integration time: 1 s for the first two panels and 2 s for the bottom panel. In all the panels, the two traces are for the tip in tunneling contact with the surface (higher intensities) and for the tip in the retracted position.
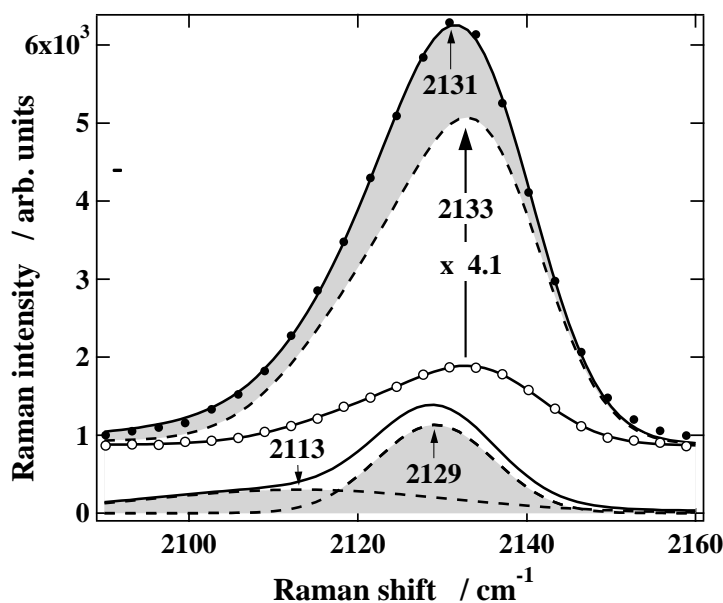
Figure 4.16: SERS and TERS spectra of the previous picture in the CN stretch region and the spectral features constituting the TERS CN stretch band (according to the fit procedure described in the text).

the EM-field. In principle, two regions can be distinguished. In the highest field region, *i.e.*, in the direct vicinity of the tip apex, only a small group of molecules on rather similar adsorption sites are affected. They will contribute to the total signal with a comparatively narrow, but strongly enhanced, Raman band. This region is denoted as region A. In regions farther out, denoted as region B, where still a considerable field enhancement is present, averaging occurs over numerous different adsorption sites. Necessarily, that leads to an inhomogeneous broadening closely comparable with that for conventional SERS sites. To illustrate this peculiar feature of combined SERS and TERS effects, Fig. 4.16 depicts a deconvolution of the observed TERS signal in the CN^- stretch region into an amplified SERS band at 2133 cm^{-1} and two asymmetric bands at 2129 cm^{-1} and 2113 cm^{-1}. The open and solid circles are the experimental data, while the solid and dashed lines represent the fit curves. The fitting procedure runs along the above described concept of two enhancement regions, denoted as A and B. The spectral shape of the latter contribution must be close to that of the SERS spectrum (where the tip

is in the retracted position). Therefore, in a first step, a fit curve for the SERS band is determined; this delivers the shape of the contribution of region B to the total TERS signal. Its amplitude is unknown. An avarage net enhancement of 4.1 is assigned to region B.[13] Subsequently, the fit program determines the amplitude, frequency and halfwidth of the remaining contributions stemming from region A. The stronger of them is a band centered at 2129 cm^{-1} having a relatively narrow halfwidth of 4.4 cm^{-1}. This band is assigned to the much smaller number of CN$^-$ ions located directly underneath the tip apex, having a more homogeneous environment. The smaller number of scatterers of this ensemble is obviously nearly compensated by a correspondingly larger near-field enhancement by the tip.

4.3   Overview on literature data concerning TERS

Few other groups have carried out TERS experiments. In the last three years, the number of experimental papers reporting successful enhancements has remained rather low, compared with the number of theoretical studies on the near-field enhancement of the Raman signal that can be found in the literature. An STM tip as an external enhancing unit has been adopted so far only in our experiments. The common alternative is an Atomic Force Microscopy (AFM) tip coated either with gold or with silver. Our approach presents the valuable advantages of fluorescence quenching and height control. On the other hand, AFM tips, commercially available[14], have extremely narrow curvature radius ($R < 10$ nm); although, the radius of the tip is increased after the deposition, usually by evaporation, of the noble metal. In Tab. 4.2 all the tip enhancements of the Raman signal that have been published are reported.

---

[13]The fit curve to the SERS data, multiplied by a factor x, is part of the total fitting procedure. It turned out that its right wing nearly matches the right wing of the TERS data if the factor is set to 4.1. A larger or smaller factor results in a mismatch of the total fit curve and experimental TERS curve.

[14]Digital Instruments GMBH, Nanosensors TappingMode Etched Silicon (TESP) probes.

Enhancing unit	Substrate	Raman scatterer	Exciting source	Observed enhancement	Net enhancement
AFM cantilever coated with silver [118]	Glass slide	Brilliant Cresyl Blue	488 nm	NR	2×10^4
Gold tip on a tuning fork [118]	Glass slide	Fullerene	488 nm	40	4×10^4
AFM cantilever coated with gold [119]	Quartz slide	Sulfur	785 nm	NR	1×10^4
STM silver tip [60]	Smooth gold film	Brilliant Cresyl Blue	633 nm	16	1×10^4
AFM cantilever coated with gold [110]	Rough silver film	Rhodamine 6G	488 nm	1.2	1×10^4
AFM cantilever coated with gold [121]	Glass slide	Polydiacetylene (PDA-PTS)	488 nm	3.4	2×10^4
AFM cantilever coated with gold [120]	Glass slide	Diamond Particle	785 nm	1.2?	NR
STM silver tip [122, 123]	Rough gold film	Cyanide	633 nm	4 / 7	$1 / 1.8 \times 10^4$

Apart from cyanide ions, all the other Raman scatterers (sulfur, diamond, dyes such as BCB or R6G, polymers) are well known for their extremely large Raman cross-sections due to high resonance effects. For low enhancement factors these molecules are better suited. Also, using a SERS active surface has been recognized as a rewarding tactic [68, 109–111].

The observed enhancement refers to the intensity gain in the recorded Raman spectra, while the effective enhancement is estimated taking in account the ratio between the laser spot size and the radius of the tip. Four orders of magnitude for the tip-enhancement is the experimental value commonly found while testing different molecules.[15] The discrepancy between experimentally achieved results and predicted enhancement factors ($10^8 - 10^{12}$) is striking. An optimal field enhancement due to the illumination of the tip requires the use of a suitable wavelength to effectively drive the plasmon modes localized in the cavity. It is peculiar that despite the different range of wavelengths used for the excitation, similar (low) factors have been obtained. Referring to Fig. 2.7, the highest field enhancement factors are expected in the near-infrared region (above 800 nm) and much weaker FEF along the tails of the main resonance. While the possibility of having a tip enhancement of the Raman signal has been experimentally demonstrated, there is, in our opinion, still scope for improvement.[16] Investigations in the near-IR may bring the desired breakthrough.

4.4 Carbon fluctuations

Spectra taken with a microprobe Raman system quite often show fast spectral fluctuations in the form of the sudden appearance and disappearance ("blinking") of rather narrow Raman lines in a wide frequency region, between 1000 cm^{-1} and 1700 cm^{-1}. Normal modes assignable to vibrations within segments of par-

---

[15]The illuminated tip amplifies the local electromagnetic field, then, comparable Raman enhancement factors should be expected, regardless of the molecular (electronic) structure.

[16]For single molecule detection tip enhancement factors $> 10^6$ are needed.

tially saturated carbon chains fall in this region. These Raman features have been observed for silver and gold electrodes, in air as well as in an electrochemical environment [124–127].

The spectra shown in Fig. 4.17, recorded continuously while directly illuminating an etched silver tip, exhibit huge fluctuations in the number, intensity and frequency of a set of narrow Raman lines appearing over a background stretching from roughly 1200 cm^{-1} to 1600 cm^{-1}. The signal for C-H stretching vibrations around 3000 cm^{-1} is also visible. The intensity of the background is also subject to fluctuation and, as for the Raman bands, it may be related to the presence of an extended carbon frame on the active surface.

The surface enhanced Raman cross section of carbonaceous molecular structures is exceptionally large, thus, very short integration times could be used, here 1 s. Still, the differences between two consecutive spectra are striking, thus pointing to the astonishing rapidity of the underlying surface processes. The seemingly random appearance of Raman lines is interpreted in terms of ongoing chemical reactions leading to the modification in the local carbon chain configuration and in the nature of the chemical bonds, involving not only carbon atoms but possibly also oxygen atoms and clearly adsorption sites on the metal surface. A feature "blinks" also at higher frequencies. It fluctuates around a central frequency of 1900 cm^{-1} and can be assigned to CO molecules adsorbed at the tip and embedded in the carbon net. The substantial frequency shift points to changes in the adsorption geometry on the metal surface and/or in the chemical surrounding of the molecule(s). The lifetime of the isolated CO group is also limited and subject to chemical rearrangement, *e.g.*, to a carbonyl group.

Summing up a large number of consecutive spectra showing significant fluctuations, an average over time is obtained. The resulting spectrum (Fig. 4.19) loses all the peculiar and narrow bands related to single well defined vibrational modes. Instead, two broad features centered at around 1300 cm^{-1} and 1500 cm^{-1} appear. These two broad envelopes of bands have been assigned, respectively, to disordered (sp^3) or graphitic (sp^2) types of carbon structures [128–130]. The intensity ratio of these two bands yields the degree of disorder within the monitored structure.
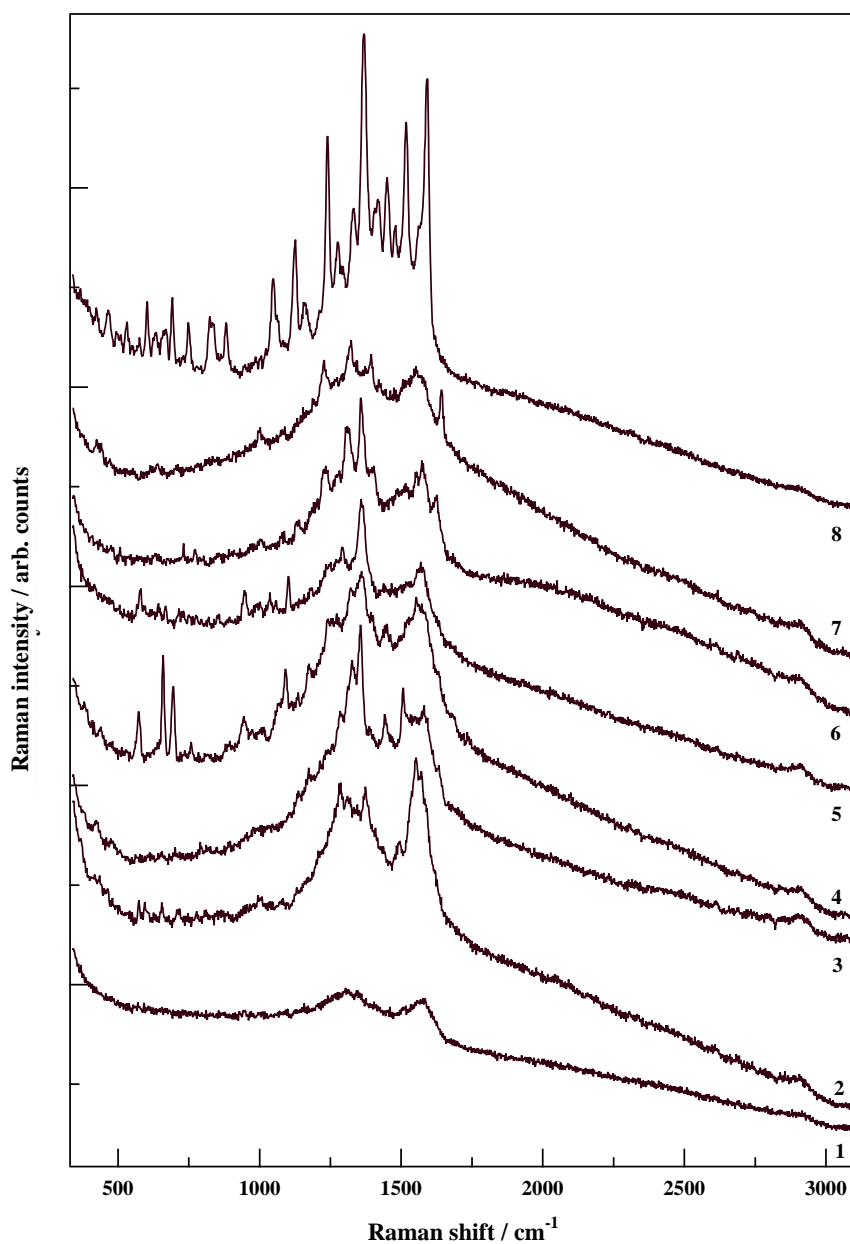
Figure 4.17: A sequence of continuously acquired Raman spectra from a carbon contaminated silver tip. Integration time for each spectrum was 1 s, with a delay time of 0.5 s, due to the mechanical opening and closing of the shutter, granting entrance to the camera detector. The spectra are artificially shifted for sake of clarity.
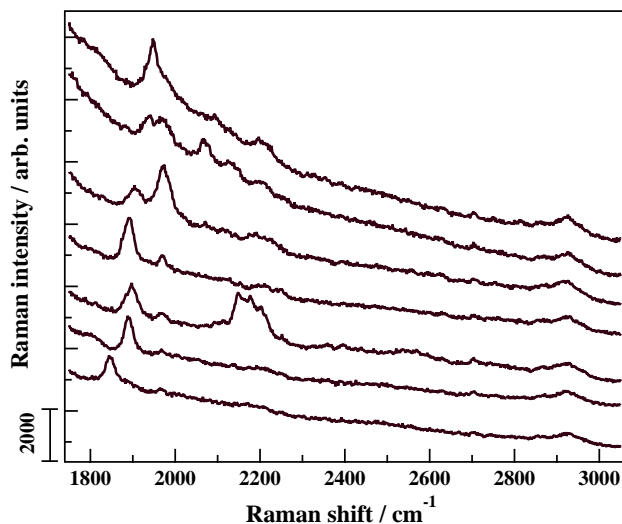
Figure 4.18: A sequence of continuously acquired Raman spectra from a silver tip in the high frequency region, showing random fluctations also for the CO stretch signal. The integration time for each spectrum was 5 s.

The D-band at lower wavenumbers is by far the most intense; hence, as expected, the carbon deposit may be considered as predominantly amorphous.

As already pointed out, only a very limited number of sub-micrometer structures on the rough metal surface actually contribute to the SER spectrum. This explains the narrowness (< 20 cm^{-1}) of the fluctuating bands: only a few segments of the carbon cluster in the vicinity of the *hot spots*, here hot spots on the tip, are probed. While the spatially inhomogeneous electromagnetic field distribution along the metal surface remains stable, the carbon network rearranges continuously, bonds are broken and new ones are formed. Some configurations may exist for a short time, which are in the optimal resonance with the exciting wavelength, thus receiving a further resonant enhancing contribution from the chemical effect and show up suddenly in the spectrum.

Even if only a few spots on the surface are actually monitored, the chemistry taking place at them, *i.e.*, the rapid fluctuations, may be considered to be representative of all the (carbon covered) area. Since the carbon deposit morphology changes continuously the spectrum obtained averaging in time over a few hot locations
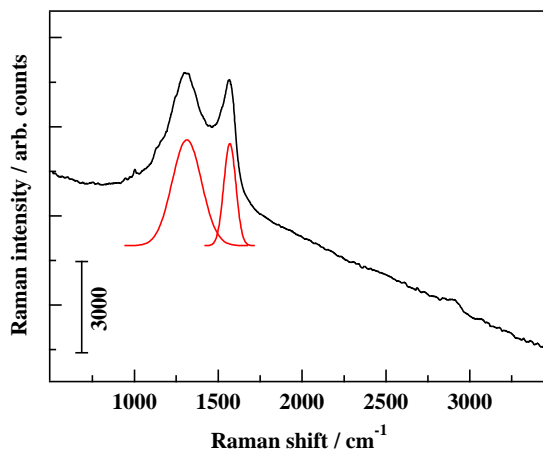
Figure 4.19: Average over 100 continuously recorded spectra from a silver tip showing intense carbon fluctuations. A deconvolution of the d peak at 1312 cm^{-1} and g peak at 1569 cm^{-1} is also shown; their intensity ratio is roughly 2.5.
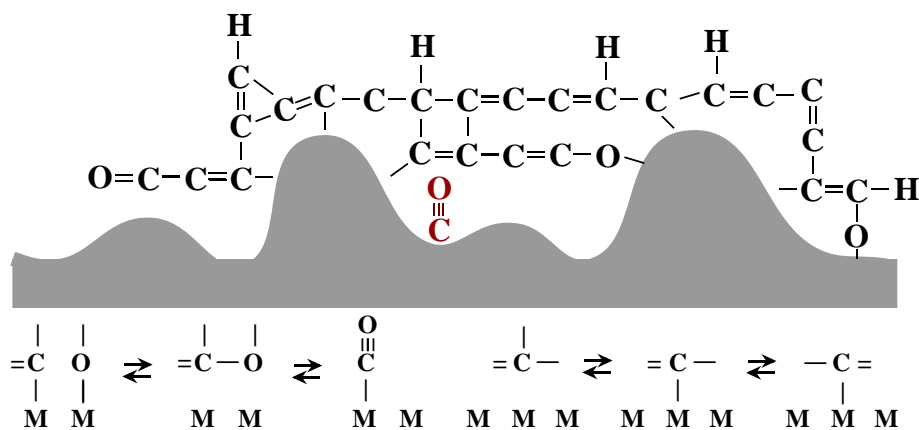

Figure 4.20: A pictorial view of the carbon spongy structure that may be formed at the rough metal surface. Possible chemical reactions taking place at different adsorbtion sites are also given.

(Fig. 4.15) corresponds indeed to an average all over the contaminated surface. The carbon presence may also be detected when performing TERS experiments (Fig. 4.16). This undesired contribution may, in the worst case, obscure the signal from the surface, especially in the 60° approach, in which not only the tip apex but, to a certain extent, also the tip side is partially illuminated. Regarding the metal film, strongly bound ions such as cyanide may prevent the direct adsorbtion of carbon to the surface. For the case of BCB, the starting signal from the uniformly adsorbed dye molecules is by far more stable and intense than the one due to impurities in trace amount and, with the sample illuminated from below through the gold film, only a very weak field extends beyond the bottom of the tip. Cleaning procedure for the tip, for example with sulfuric acid, may be applied, but to eliminate completely any possible carbon contamination from the air is very difficult [131].